

Revision of adsorption models of xyloglucan on microcrystalline cellulose

Dawid Myśliwiec · Monika Chylińska ·
Monika Szymańska-Chargot ·
Stanisław Chibowski · Artur Zdunek

Received: 30 March 2016 / Accepted: 24 June 2016 / Published online: 6 July 2016
© The Author(s) 2016. This article is published with open access at Springerlink.com

Abstract Interactions among cellulose, hemicellulose and pectins are important for plant cell wall assembly and properties and also for industrial applications of these polysaccharides. Therefore, binding of pectin and xyloglucan on microcrystalline cellulose was investigated in this experiment by adsorption isotherms, zeta potential and scanning electron microscopy (SEM). Analysis of three isotherm models (Langmuir, Freundlich and Fowler-Guggenheim isotherms) showed that the experimental adsorption isotherm was well described via the Fowler-Guggenheim model, which includes lateral interaction between the adsorbate. The adsorption isotherm and zeta potential measurement showed that at temperature 25 °C only xyloglucan adsorbed on the microcrystalline cellulose. In case of xyloglucan on cellulose, the equilibrium was reached in about 3–4 h, and the kinetics of adsorption were well described by the multiexponential equation. Analysis of the model suggests that two steps can be distinguished: diffusion and reformation in an adsorbed

layer. No adsorption of pectin was observed in this study. SEM study showed that xyloglucan may prevent cellulose from aggregation.

Keywords Adsorption · Cellulose · Pectin · Xyloglucan · Kinetics · Equilibrium

Introduction

Cellulose consists of an unbranched polymer chain of β -(1 \rightarrow 4)-linked glucose residues. In the native cellulose crystallites, the molecules have a flat ribbon shape with intramolecular hydrogen bonds, and they cohere owing to intermolecular van der Waals and hydrogen bonding interactions. In nature, these molecules are often grouped into clusters (elementary fibrils) of 18 or more chains. The clusters can diffract an X-ray beam and are therefore considered to be crystalline. The glucan chain length (degree of polymerization) varies from about 2000 to more than 25,000 glucose residues (Cousins and Brown 1995; Brown et al. 1996). These chains are long enough (about 1–12.5 μ m long) to extend through multiple crystalline and amorphous regions within a microfibril (Taiz and Zeiger 2002).

The hemicellulose xyloglucan (XyG) is found in the cell walls of all vascular plants and is the major hemicellulose in the primary cell wall of dicotyledons, where it is believed to play an important role in cell

D. Myśliwiec · S. Chibowski
Department of Radiochemistry and Colloid Chemistry,
Faculty of Chemistry, Maria Curie-Skłodowska
University, Maria Curie-Skłodowska Sq. 3, 20031 Lublin,
Poland

M. Chylińska · M. Szymańska-Chargot (✉) · A. Zdunek
Institute of Agrophysics, Polish Academy of Sciences,
Doświadczalna 4, 20-290 Lublin, Poland
e-mail: m.szymanska@ipan.lublin.pl

wall structure and function (Taiz and Zeiger 2002; Eckardt 2008). Like cellulose, this polysaccharide has a backbone composed of (1 → 4)-linked β -D-glucose residues. Additionally, it has short side chains of xylose, galactose and often but not always a terminal fucose or arabinose, which prevent the assembly of xyloglucan into a crystalline cellulose-like microfibril. Tamarind xyloglucan is an example of non-fucosylated storage xyloglucan (Zykwinska et al. 2008; Kozioł et al. 2015), and its molar mass is estimated at 763 kDa (Zykwinska et al. 2005). The conformation may partially resemble a flat ribbon, which is thought to be able to create hydrogen bond to the similar β -glucan chains of cellulose on the surface of the microfibril (Albersheim et al. 2011). Moreover, some XG molecules may penetrate and disrupt the microcrystalline parts of cellulose molecules (Pauly et al. 1999).

Pectins together with hemicelluloses are matrix components of the primary cell wall; they can be extremely heterogeneous between plants and tissues and even within a single cell wall. Three major pectic polysaccharides are known: homogalacturonan (HG), rhamnogalacturonan I (RGI) and rhamnogalacturonan II (RGII). Their backbones and side chains contain acidic sugars and neutral sugars (Taiz and Zeiger 2002; Willats et al. 2006).

According to the common plant cell wall model, the cellulose is organized in microfibrils, which are tethered and connected via hemicelluloses. Recent findings suggest that only a very minor part of hemicelluloses, i.e., xyloglucan, would be in tight interactions with the cellulose crystalline structure (Park and Cosgrove 2015). The cellulose–xyloglucan network is embedded in a highly hydrated matrix composed of pectin and other hemicelluloses (Carpita and Gibaut 1993). The cellulose–xyloglucan network constitutes the major load-bearing structure of the primary cell wall (Keegstra et al. 1973; Verbelen and Vissenberg 2007). It is also thought to act as a spacer preventing cellulose microfibrils from aggregating (Thompson 2005). However, the picture of interactions between the cellulose and non-cellulosic polysaccharides is still unclear.

In the literature cellulose is reported among many others as an adsorbate of starch (Guan et al. 2008), lignin (Maximova et al. 2001) or chlorhexidine (Giménez-Martín et al. 2009). Previous investigations of pectin and hemicellulose adsorption on cellulose

microfibrils have already been conducted (Zykwinska et al. 2008), but all experiments were done at 40 °C, which may not correspond to the conditions that might be found in environmental systems. Also, Langmuir or Freundlich models are currently favored for adsorption of xyloglucan onto cellulose (Zykwinska et al. 2008). Therefore, the aim of the present study was to determine whether the adsorption of either citrus-apple pectin or xyloglucan on the microcrystalline cellulose takes place under mild conditions similar to those occurring in nature. The mechanism of adsorption of xyloglucan molecules onto cellulose was investigated and revised as well. Results of adsorption isotherms were analyzed considering the Langmuir, Freundlich and Fowler-Guggenheim models.

Materials

Commercially available polysaccharides were used in the experiment. Microcrystalline cellulose Avicel PH-101 was purchased from FMC Biopolymer (Belgium) with the average crystal size of 50 μ m. Xyloglucan (tamarind, purity ~95 %, molecular weight: 225 kD (MALS) with sugar composition: xylose, 34 %; glucose, 45 %; galactose, 18 %; arabinose, 3 %) was from Megazyme (Bray, Ireland). Highly esterified citrus-apple pectin with esterification degree 59.3 % and galacturonic acid content of 428 mg/g of pectins was from Pektowin (Jasło, Poland).

Cellulose was purified by boiling twice in deionized water for 3 h. The xyloglucan and citrus-apple pectin were used without further purification.

Methods

Adsorption experiment

All experiments were carried out at room temperature (25 ± 1 °C). The pH of the solutions was monitored by adding phosphate buffer (pH 6.9, $I = 0.1$); 0.50 g of cellulose was added to the 25 ml of pectin and xyloglucan solutions of different concentrations. Suspensions were shaken during the entire process (200 rpm/min). The time required for reaching the equilibrium condition was estimated by drawing samples at intervals of time until equilibrium was reached. Suspensions were filtered through syringe filters (Chromafil GF/PET-45/25), and

1 ml of clear solution was taken for determination of the concentration of carbohydrates (pectins and xyloglucan). Different initial concentrations of pectin and xyloglucan solutions were prepared by proper dilution from stock solutions with concentrations of 200 and 150 ppm, respectively. Each point of the isotherm is an average from three independent replicates.

The carbohydrate content was determined by the sulfuric acid-UV method as follows (Albalasmeh et al. 2013). A 1 ml aliquot of carbohydrate solution was mixed with 3 ml concentrated sulfuric acid in a test tube and vortexed for 30 s. The temperature of the mixture rose rapidly within 10–15 s after addition of sulfuric acid. Then, the solution was cooled in ice for 2 min to bring it to room temperature. Finally, UV light absorption at 315 nm was read using a UV spectrophotometer. Solutions for the calibration curve were prepared following the same procedure as above.

The specific surface area of cellulose was determined via the low-temperature nitrogen adsorption isotherm measured with ASAP 2405 from Micromeritics Inc. The results demonstrate that this value is lower than $1 \text{ m}^2/\text{g}$, which suggests no porosity, and therefore it is better to express the adsorbed amount in mg/g than mg/m^2 . Moreover, the very low specific surface area suggests that the cellulose is bundled with other cellulose microfibrils leaving little space for adsorption.

Examination of the microstructure by scanning electron microscope (SEM)

Morphology of polysaccharides was examined by scanning electron microscope (SEM, Quanta 3D FEG, FEI Phenom Word). Prior to SEM observation, the samples were air dried and coated with an ultrathin layer of gold in an ion sputtering machine.

Zeta potential measurements

Zeta potential was measured with Zetasizer nano ZS-90 (Malvern) using the dip-cell system. The suspension concentration was equal to 1 g/l ; 50 ml of a suspension was poured into a flask, and the pH was set by adding controlled volumes of 0.1 M NaOH and 0.1 M HCl solutions. When a stable pH had been achieved, an appropriate volume of 1 M NaCl solution was added in order to obtain the ionic strength of the suspension (equal to 0.25). Prior to all measurements, the suspension was sonicated for 3 min to ensure

maximum homogeneity; 0.8 ml of a suspension was pipetted to a cuvette and thermostated for 120 s. Measurement involved 30 runs. Each experimental point is a mean value of at least four independent replicates. The concentration of xyloglucan and pectins in suspension was equal to 10 ppm when their influence on the zeta potential was investigated.

Adsorption models

Experimental data were fitted to three most commonly used models of isotherms:

$$a = a_m \frac{kc}{1 + kc} \quad (1)$$

$$a = kc^{1/n} \quad (2)$$

$$a = a_m \frac{kc \exp(\alpha a/a_m)}{1 + kc \exp(\alpha a/a_m)} \quad (3)$$

In all Eqs. (1)–(3), k is an adsorption constant of the process, a_m is the maximum adsorption (adsorption capacity), c stands for the equilibrium concentration, and α is a constant that describes interactions between molecules in the adsorbed layer. Equation (1) was proposed by Langmuir (1918) and assumes that adsorbed molecules of adsorbate interact only with adsorption sites on the solid surface. Equation (2) is a purely empirical isotherm proposed by Freundlich (Chang et al. 2000). Equation (3) is a Fowler-Guggenheim isotherm that takes into account lateral interactions between adsorbed molecules (Hamdaoui and Naffrechoux 2007). Equation (3) reduces to a Langmuir isotherm (Eq. 1), when there are no lateral interactions ($\alpha = 0$).

Statistical analysis

Measurement uncertainty was calculated with a statistical approach based on at least four independent replicates (Konieczka and Namieśnik 2007):

$$\text{MU} = \frac{\text{SD}}{\sqrt{n}} \times t_{0.05;n-1} \quad (4)$$

where MU is measurement uncertainty, SD stands for standard deviation, n is a number of replicates, and $t_{0.05;n-1}$ is the parameter of the t-Student distribution. Grubbs test for outliers was performed before the uncertainty was calculated (Konieczka and Namieśnik 2007).

Linear forms of the isotherm models (Eqs. 1–3) were not considered in this manuscript (El-Khaiary and Malash 2011). Goodness of the fit was justified by the following conditions: the expected value of errors is zero (Walesiuk and Gantar 2012); errors are homoscedastic, which means that they have constant variance (Chatterjee and Simonoff 2013); errors are normally distributed and uncorrelated (Walesiuk and Gantar 2012).

In order to estimate how well the model explains the experimental data, besides the R^2 parameter, the adjusted version (R_a^2 , which takes into account the number of parameters), the chi-squared statistic (χ^2) and both the Akaike informational criterion (AIC) and corrected Akaike informational criterion (AIC_{corr} , which takes into account the number of parameters) were taken into consideration. The following equations were used to calculate those values (El-Khaiary 2008; Danish et al. 2011; Turner et al. 2015):

$$R_a^2 = R^2 - p(1 - R^2)/(n - p - 1) \quad (5)$$

$$\chi^2 = \sum \frac{(a_e - a_t)^2}{a_t} \quad (6)$$

$$AIC = N \ln \left(\frac{\sum (a_e - a_t)^2}{n} \right) + 2p \quad (7)$$

$$AIC_{corr} = AIC + \frac{2p(p+1)}{n-p-1} \quad (8)$$

where p and n stand for the number of parameters of the model and number of experimental data points, respectively. The a stands for adsorption, subscripts e and t for its experimental and theoretical (calculated from the model) value.

Results and discussion

Adsorption kinetics

Adsorption kinetics data are shown in Fig. 1a. The results show that xyloglucan adsorbed on cellulose while no sorption was observed for pectin, although the experiment was conducted for 72 h. Moreover, equilibrium was reached for xyloglucan after approximately 3–4 h. A brief analysis of the kinetics may give some insights into the mechanism of the process,

as has been shown in numerous papers (Bonifazi et al. 1996; Marczewski 2007, 2010, 2011; Deryło-Marczewska et al. 2010; Marczewski et al. 2013).

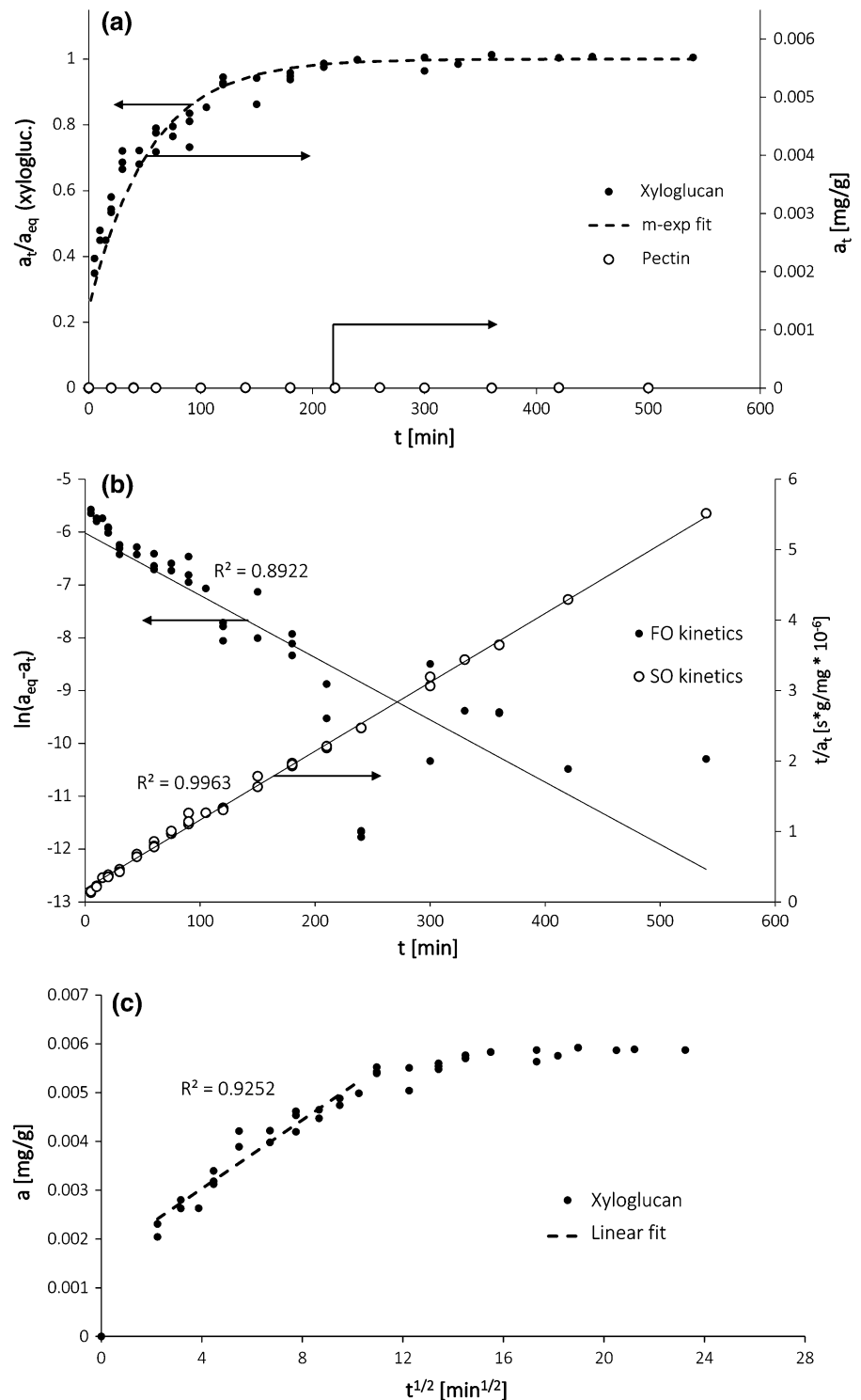
The commonly applied procedure concerning adsorption kinetics data analysis is an application of the first order (FO) and second order (SO) kinetic equation in linear forms as it was depicted in Fig. 1b, e.g., the Lagergren plot for the FO equation (Akmil-Basar et al. 2005; Marczewski 2010): $\ln(a_t - a_{eq})$ versus t and t/a_t versus t for the SO equation where a_t stands for adsorption at time t and a_{eq} for the amount adsorbed in equilibrium. However, such a method requires data transformation, which may lead to further transformation of data deviation (Draper and Smith 1998; Carroll et al. 2006; Chatterjee and Simonoff 2013). Therefore, in this study, fitting data to linear forms of FO and SO was done only to evaluate the equilibrium adsorption value used in further analysis with a multiexponential equation (to calculate the adsorption progress precisely).

The transformed data fitted much better to the SO equation ($R^2 = 0.996$) as was shown in Fig. 1b. Therefore, the equilibrium adsorption value was calculated using this model. Further analysis of the kinetics of the process involved a multiexponential equation, which allowed representing the whole adsorption kinetics as a linear combination of several first order processes (Deryło-Marczewska et al. 2010; Bonifazi et al. 1996; Marczewski 2011):

$$F = 1 - \sum_i f_i \exp(-k_i t), \quad (9)$$

where F is the adsorption progress (fractional attainment of equilibrium, a_t/a_{eq}), f_i is the contribution of the i th process in total adsorption, and k_i is the kinetic constant of an i th process; t stands for time. Results are presented in Fig. 3. In the present calculations, the three components were used; however, it was determined that only two of them were required to describe data sufficiently well. Calculations showed that 0.243 of a total adsorption may be explained by the fast process ($k_1 = 0.072 \text{ s}^{-1}$), and 0.757 of the entire adsorption is contributed to a slow process ($k_2 = 3.09 \times 10^{-3} \text{ s}^{-1}$). Figure 1c presents the Weber-Morris plot on which the presence of linear region suggests that intraparticle diffusion might be one of these processes (Wasewar et al. 2008; Płaziński and Rudziński 2009). However, the specific cellulose structure, for example, specific surface area $<1 \text{ sq. m/}$

Fig. 1 Adsorption kinetics data: **a** kinetics of the xyloglucan and pectin adsorption—concentration/adsorption progress versus time; **b** linear fits of experimental data of xyloglucan adsorption to linear forms of the FO and SO kinetic equation; **c** Weber-Morris plot of xyloglucan adsorption



g (measured by low temperature nitrogen adsorption), suggests that the mechanism could be slightly different here. As was shown, the high content of cellulose

in the suspension may result in an inhibition of mass transfer in the system (Roberts et al. 2011). Therefore, the structure of the cellulose in the suspension in some

way mimics a complex pore structure of adsorbents with higher surface area, e.g., activated carbons. An important argument in favor of such a statement is the fact that polymeric molecules with high molecular mass, such as xyloglucan, would be more susceptible to a proposed adsorption mechanism.

The other process that might play a significant role in the total adsorption rate is reconfiguration (sometimes called relaxation) of a polymer (in this case xyloglucan) in the adsorbed layer (Scheutjens and Fleer 1979; Shulga et al. 2003; Patkowski et al. 2014). When most of the available surface is coated with xyloglucan, a new free surface available for the ‘bulk’ polymer molecules to adsorb may be created only after macromolecules in the adsorbed layer have changed their structure to a more compact one. This may happen by creating more loops (which decreases amount of trains) or by desorption and almost instant adsorption of the same molecule in a different structure, which requires less surface area on a cellulose fiber (Patkowski et al. 2014). This hypothesis is strongly supported by the equilibrium adsorption data, which will be discussed further in this article.

The two-step adsorption mechanism of xyloglucan on cellulose was previously proposed by some authors (Pirich et al. 2015; Villares et al. 2015; Dammak et al. 2015). Moreover, Winter et al. (Winter et al. 2010) showed that the stability of the bacterial cellulose nanocrystal suspension increases above a certain concentration ratio of xyloglucan, which may be due to a change in the dominant molecule conformation on the surface. Villares et al. postulated that for a low bulk xyloglucan concentration adsorption (driven by diffusion), the kinetics constant is comparable to the reconfiguration kinetics constant. For higher bulk concentrations (and thus higher adsorbed amounts), the reconfiguration constant decreases and reconfiguration becomes a limiting stage of the process. The mechanism proposed in this article is very similar. During the equilibration, two processes occur that limit the total kinetics of adsorption. These processes are most likely diffusion and reconfiguration. The analysis of the presented data and findings of Villares et al. (2015) allow us to postulate that the fast process (which contributes to 0.243 of the total adsorption kinetics) is a diffusion through a dense cellulose suspension and/or surface diffusion in the adsorbed layer, and the limiting and dominant one (explaining 0.757 of adsorption) is reconfiguration of molecules in

the adsorbed layer. The fast process most likely occurs when the locally surface concentration of xyloglucan (adsorption) is low. So even for a high bulk concentration of xyloglucan, the net mechanism is a combination of two processes. However, further studies are needed to exclude other possibilities and examine whether the adsorption of xyloglucan on cellulose is assisted by some chemical reactions (e.g., during reconfiguration or sorption itself).

Adsorption equilibrium

Adsorption equilibrium data obtained for the Langmuir and Fowler-Guggenheim isotherms are shown in Fig. 2. This result confirms that only xyloglucan adsorbs on cellulose in the chosen experimental conditions. In order to avoid error transformations (Draper and Smith 1998; Carroll et al. 2006; Chatterjee and Simonoff 2013), the experimental data were fitted directly to nonlinear forms of the Langmuir, Freundlich and Fowler-Guggenheim isotherms; see Eqs. (1)–(3). The statistical tests were performed to choose the best fitted isotherms. Results are presented in Table 1. A Fowler-Guggenheim adsorption was the best to describe adsorption in the studied system (see also Fig. 2), even despite the fact that it has more parameters that were found by adjustment of R_a^2 and AIC_{corr} . Therefore, this is evidence that lateral interactions play an important role in the adsorption of xyloglucan on cellulose. This result also confirms that chain-chain interactions as well as xyloglucan reconfiguration was probably a process that could limit the adsorption kinetics, as was mentioned above. It is also worth noticing that some authors (Pirich et al. 2015) compared the Freundlich and Langmuir model when describing the adsorption of xyloglucan on cellulose. However, none of these two models is able to include lateral interactions in the adsorbed layer, which were proposed in the literature (Pirich et al. 2015; Dammak et al. 2015). Therefore, in future analysis, the Fowler-Guggenheim model and its parameters may help in the qualitative and quantitative description of the adsorption of xyloglucan on cellulose.

Zeta potential

The zeta potentials of the system are shown in Fig. 3. Any difference in the zeta value in comparison to the control system without the adsorbate was a result of

Fig. 2 Adsorption isotherms of xyloglucan and pectin on cellulose with fitted Fowler-Guggenheim and Langmuir isotherms

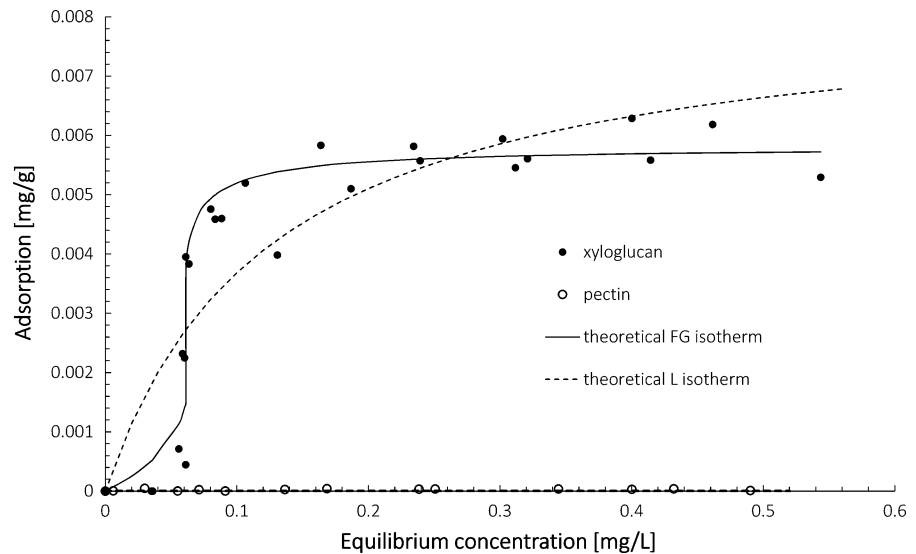


Table 1 Fitting experimental data to theoretical models

		Fowler-Guggenheim isotherm		Langmuir isotherm		Freundlich isotherm	
Parameters ^a		α	4.26	a_m	7.98	k	0.009
		a_m	5.81	k	8.303	n	2.24
		k	1.89				
Goodness of fit	AIC ^{b,c}	33.14		89.68		96.76	
	AIC _{cor} ^c	34.23		90.21		97.27	
	R^2	0.9688		0.7273		0.6456	
	R_a^2	0.9659		0.7025		0.6134	
	χ^2 ^c	1.549		11.91		14.36	
Properties of residuals ^d (p values)	$S-W$	0.1696		0.2539		0.0998	
	$G-Q$ versus a	0.9469		0.5077		0.2042	
	$G-Q$ versus c	0.0166*		0.0378*		0.0202*	

* Value is statistically significant at 95 % CI, meaning that those distributions are not homoscedastic

^a Monolayer capacity (a_m) in ($\mu\text{g/g}$), k constant in (l/mg); others are dimensionless

^b Akaike information criterion

^c Lower is better

^d $S-W$ Shapiro-Wilk test for normality, $G-Q$ Goldfeld-Quandt test for homoscedasticity; a and c stand for the adsorption and equilibrium concentration, respectively

either incorporation of a charge into a diffused layer or a shift of the slipping plane (Grządka 2015). Both mentioned processes were results of adsorption; therefore, the change in zeta potential of cellulose dispersion in the presence of xyloglucan and no change in a wide pH range in case of pectin confirmed the previous observation that pectin did not adsorb on cellulose in the studied system.

SEM image analysis

Since there was no pectins adsorption onto cellulose, only the SEM images of cellulose, xyloglucan and the cellulose after adsorption of xyloglucan in two magnifications are presented in Fig. 4. The cellulose has a natural tendency to aggregate (Fig. 4a, e), while the xyloglucan was smaller compared with cellulose

Fig. 3 Zeta potential versus pH plot for the cellulose suspension, cellulose suspension in the presence of 10 ppm xyloglucan and cellulose in the presence of the 10 ppm pectin suspension

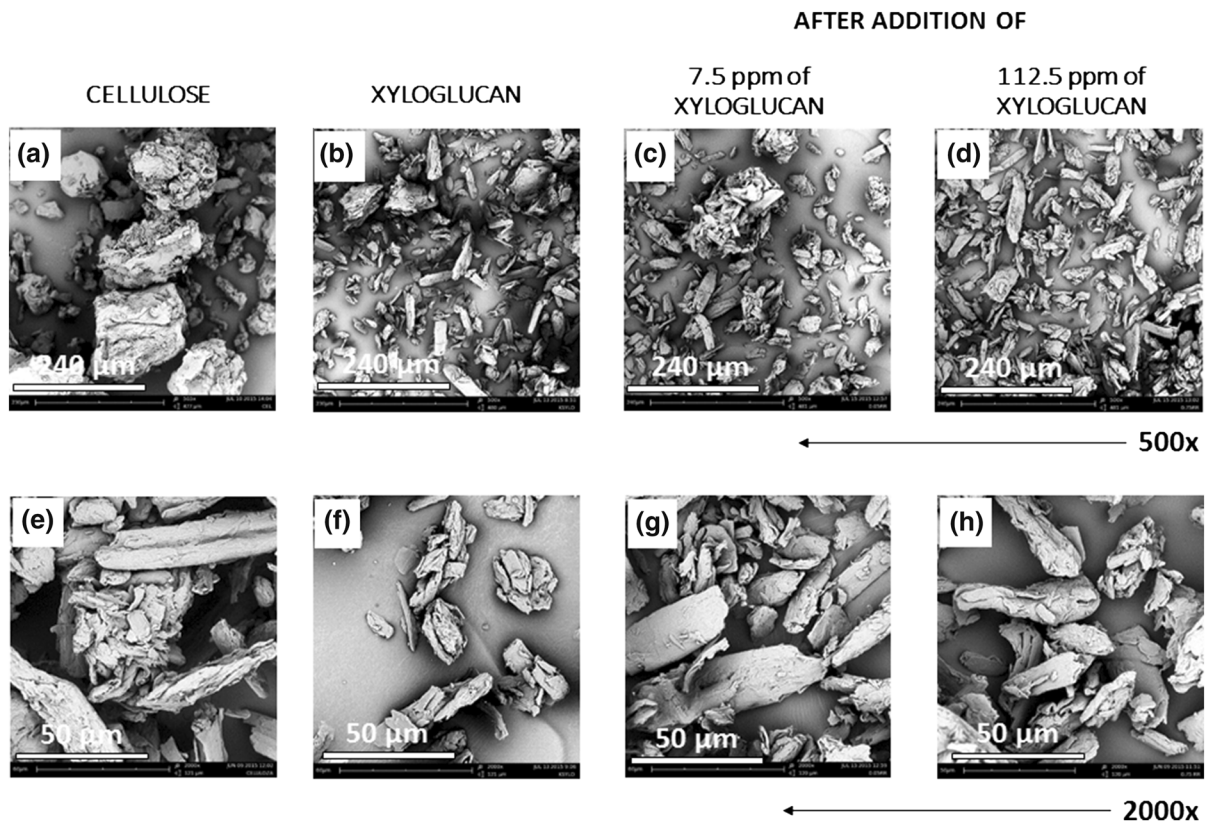
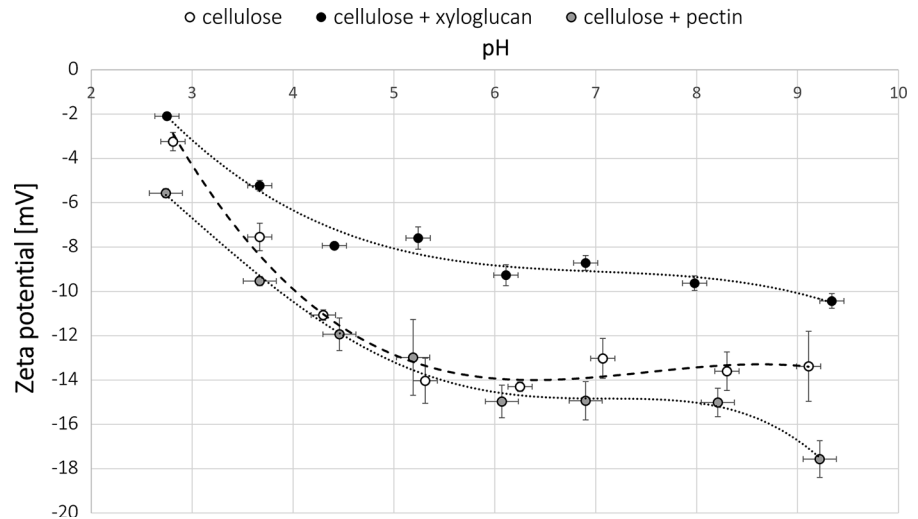


Fig. 4 SEM images of cellulose (a, e), xyloglucan (b, f) and cellulose after adsorption of xyloglucan from aqueous solution of the given initial concentration (c, d, g, h); magnification: $\times 500$ (a–d) and $\times 2000$ (e–h)

(Fig. 4b, f). In the adsorption experiment, after the addition of 7.5 ppm of xyloglucan, the SEM images showed the cellulose still had a tendency to aggregate,

and the aggregates were surrounded by the smaller xyloglucan (Fig. 4c, g). However, after addition of 112.5 ppm, there was no further evidence of cellulose

aggregation (Fig. 4d, h), which is in accordance with the results obtained from the atomic force microscope for celery (*Apium graveolens*) cell walls in which the removal of xyloglucan and pectins induced the cellulose microfibrils to self-associate and aggregate (Thimm et al. 2002, 2009). The recent findings suggest that xyloglucan plays the role of the molecular binder and is involved in the adhesion of microfibrils over short distances (Cosgrove and Jarvis 2012; Park and Cosgrove 2012).

In the present study, Avicel cellulose was used, which is highly crystalline (53.8 %) and mostly contains the I β structure (96 %) (Szymańska-Chargot et al. 2011). Chambat et al. (2005) showed the different cellulose structures, for which the crystallinity and specific surface area are key factors that potentially influence xyloglucan binding. Because the effective surface area for binding varies with xyloglucan size, the binding kinetics are complicated and partly limited by size-dependent xyloglucan diffusion into the pores of the particles (Park and Cosgrove 2015). During cell wall formation, the xyloglucan probably is not only connected with the cellulose microfibrils via hydrogen bonding but also physically interwoven into them (Pauly et al. 1999).

Conclusions

The adsorption kinetics and zeta potential measurements confirmed that only xyloglucan adsorption on microcrystalline cellulose occurs, while adsorption of pectins was not observed. In the case of the xyloglucan/cellulose system, equilibrium was reached after approximately 3–4 h. Multiexponential analysis of the adsorption kinetics suggests that two components influenced the process. We postulate that these were diffusion of an adsorbate through the dense cellulose suspension and reformation in an adsorbed layer, which means that interactions between xyloglucan chains play an important role in total adsorption. Since xyloglucan adsorption was well described by the Fowler-Guggenheim isotherm, the lateral interactions in an adsorbed layer play an important role. Moreover, the presence of xyloglucan in the cellulose suspension increased the zeta potential in a wide range of pH. Because this may be attributed to at least two phenomenon, namely shift of the slipping plane and incorporation of a charge in an adsorbed layer, the

only conclusion that can be made is that xyloglucan adsorbs on cellulose.

Acknowledgments The study was supported under project no. 2011/01/D/NZ9/02494 funded by The Polish National Science Centre Poland (NCN).

Open Access This article is distributed under the terms of the Creative Commons Attribution 4.0 International License (<http://creativecommons.org/licenses/by/4.0/>), which permits unrestricted use, distribution, and reproduction in any medium, provided you give appropriate credit to the original author(s) and the source, provide a link to the Creative Commons license, and indicate if changes were made.

References

- Akmil-Başar C, Önal Y, Kiliçer T, Eren D (2005) Adsorptions of high concentration malachite green by two activated carbons having different porous structures. *J Hazard Mater* 127:73–80
- Albalasmeh AA, Berhe AA, Ghezzehei TA (2013) A new method for rapid determination of carbohydrate and total carbon concentrations using UV spectrophotometry. *Carbohydr Polym* 97:253–261
- Albersheim P, Darvill A, Roberts K, Sederoff R, Staehelin A (2011) Plant cell walls. *Gerland sciences*. Taylor & Francis, London
- Bonifazi M, Pant BC, Langford CH (1996) Kinetic study of speciation of copper(II) bound to humic acid. *Environ Technol* 17:885–890
- Brown RM Jr, Saxena IM, Kudlicka K (1996) Cellulose biosynthesis in higher plants. *Trends Plant Sci* 1:149–155
- Carpita NC, Gibaut DM (1993) Structural models of primary cell walls in flowering plants: consistency of molecular structure with the physical properties of the walls during growth. *Plant J* 3:1–30
- Carroll RJ, Ruppert D, Stefanski LA, Crainiceanu CM (2006) Measurement error in nonlinear models. A modern perspective. Chapman & Hall/CRC, London
- Chambat G, Karmous M, Costes M, Picard M, Joseleau JP (2005) Variation of xyloglucan substitution pattern affects the sorption on celluloses with different degrees of crystallinity. *Cellulose* 12:117–125
- Chang HT, Furuya EG, Miura Y, Noll KE (2000) Effect of surface functional group on Freundlich adsorption isotherm. *Water Sci Technol* 42:161–166
- Chatterjee S, Simonoff JS (2013) Handbook of regression analysis. Wiley, New York
- Cosgrove DJ, Jarvis MC (2012) Comparative structure and biomechanics of plant primary and secondary cell walls. *Front Plant Sci* 3(1–6):204
- Cousins SK, Brown RM Jr (1995) Cellulose I microfibril assembly: computational molecular mechanics energy analysis favors bonding by van der Waals forces as the initial step in crystallization. *Polymer* 36:3885–3888
- Dammak A, Quémener B, Bonnin E, Alvarado C, Bouchet B, Villares A, Moreau C, Cathala B (2015) Exploring

- architecture of xyloglucan cellulose nanocrystal complexes through enzyme susceptibility at different adsorption regimes. *Biomacromolecules* 16:589–596
- Danish M, Hashim R, Rafatullah M, Sulaiman O, Ahmad A, Govind A (2011) Adsorption of Pb(II) Ions from aqueous solutions by date bead carbon activated with ZnCl₂. *Clean Soil Air Water* 39:392–399
- Deryło-Marczewska A, Mirosław K, Marczewski AW, Sternik D (2010) Studies of adsorption equilibria and kinetics of o-, m-, p-nitro- and chlorophenols on microporous carbons from aqueous solutions. *Adsorption* 16:359–375
- Draper NR, Smith H (1998) *Applied regression analysis*. Wiley, New York
- Eckardt NA (2008) Role of xyloglucan in primary cell walls. *Plant Cell* 6:1421–1422
- El-Khaiary MI (2008) Least square regression of adsorption equilibrium data: comparing the options. *J Hazard Mater* 158:73–87
- El-Khaiary MI, Malash GF (2011) Common data analysis errors in batch adsorption studies. *Hydrometallurgy* 105:314–320
- Giménez-Martín E, López-Andrade M, Ontiveros-Ortega A, Espinosa-Jiménez M (2009) Adsorption of chlorhexidine onto cellulosic fibers. *Cellulose* 3:467–479
- Grządka E (2015) Adsorption and electrokinetic properties in the system: beta-cyclodextrin/alumina in the presence of ionic and non-ionic surfactants. *Colloids Surf A* 481:261–268
- Guan Y, Qian L, Xiao H, Zheng A, He B (2008) Synthesis of a novel antimicrobial-modified starch and its adsorption on cellulose fibers: part II—adsorption behaviors of cationic starch on cellulose fibers. *Cellulose* 4:619–629
- Hamdaoui O, Naffrechoux E (2007) Modeling of adsorption isotherms of phenol and chlorophenols onto granular activated carbon. Part I. Two-parameter models and equations allowing determination of thermodynamic parameters. *J Hazard Mater* 147:381–394
- Keegstra K, Talmadge KW, Bauer WD, Albersheim P (1973) The structure of plant cell walls. III. A model of the walls of suspension-cultured sycamore cells based on the interconnections of the macromolecular components. *Plant Physiol* 51:188–196
- Konieczka P, Namieśnik J (2007) *Ocena i Kontrola Jakości Wyników Pomiarów Analitycznych*. Wydawnictwo Naukowo-Techniczne, Warszawa
- Kozioł A, Cybulska J, Pieczywek PM, Zdunek A (2015) Evaluation of structure and assembly of xyloglucan from tamarind seed (*Tamarindus indica* L.) with atomic force microscopy. *Food Biophys* 4:396–402
- Langmuir I (1918) The adsorption of gases on plane surfaces of glass, mica and platinum. *J Am Chem Soc* 40(9):1361–1403
- Marczewski AW (2007) Kinetics and equilibrium of adsorption of organic solutes on mesoporous carbons. *Appl Surf Sci* 253:5818–5826
- Marczewski AW (2010) Application of mixed order rate equations to adsorption of methylene blue on mesoporous carbons. *Appl Surf Sci* 256:5145–5152
- Marczewski AW (2011) Extension of Langmuir kinetics in dilute solutions to include lateral interactions according to regular solution theory and the Kiselev association model. *J Colloid Interface Sci* 361:603–611
- Marczewski AW, Deryło-Marczewska A, Słota A (2013) Adsorption and desorption kinetics of benzene derivatives on mesoporous carbons. *Adsorption* 19:391–406
- Maximova N, Österberg M, Koljonen K, Stenius P (2001) Lignin adsorption on cellulose fibre surfaces: effect on surface chemistry, surface morphology and paper strength. *Cellulose* 2:113–125
- Park YB, Cosgrove DJ (2012) A revised architecture of primary cell walls based on biochemical changes induced by substrate-specific endoglucanases. *Plant Physiol* 158:1933–1943
- Park YB, Cosgrove DJ (2015) Xyloglucan and its interactions with other components of the growing cell wall. *Plant Cell Physiol* 56:180–194
- Patkowski J, Myśliwiec D, Chibowski S (2014) Adsorption of polyethyleneimine (PEI) on hematite. Influence of magnetic field on adsorption of PEI on hematite. *Mater Chem Phys* 144:451–461
- Pauly M, Albersheim P, Darvill A, York WS (1999) Molecular domains of the cellulose/xyloglucan network in the cell wall of higher plants. *Plant J* 20:629–639
- Pirich CL, Freitas RA, Woehl GF, Picheth GF, Petri DFS, Sierakowski MR (2015) Bacterial cellulose nanocrystals: impact of the sulfate content on the interaction with xyloglucan. *Cellulose* 22:1773–1787
- Plaziński W, Rudziński W (2009) Kinetics of adsorption at solid/solution interfaces controlled by intraparticle diffusion: a theoretical analysis. *J Phys Chem C* 113:12495–12501
- Roberts KM, Lavenson DM, Tozzi EJ, McCarthy MJ, Jeoh T (2011) The effects of water interactions in cellulose suspensions on mass transfer and saccharification efficiency at high solids loadings. *Cellulose* 18:759–773
- Scheutjens JMHM, Fleer GJ (1979) Statistical theory of the adsorption of interacting chain molecules. I. Partition function, segment density distribution, and adsorption isotherms. *J Phys Chem* 83:1619–1635
- Shulga A, Widmaier J, Pefferkorn E, Champ S, Auweter H (2003) Kinetics of adsorption of polyvinylamine on cellulose fibers. I. Adsorption from salt-free solutions. *J Colloid Interface Sci* 258:219–227
- Szymańska-Chargot M, Cybulska J, Zdunek A (2011) Sensing the structural differences in cellulose from apple and bacterial cell wall materials by Raman and FT-IR spectroscopy. *Sensors* 11:5543–5560
- Taiz L, Zeiger E (2002) *Plant physiology*, 3rd edn. Sinauer Associates, Sunderland
- Thimm JC, Burritt DJ, Sims IM, Newman RH, Ducker WA, Melton LD (2002) Celery (*Apium graveolens*) parenchyma cell walls: cell walls with minimal xyloglucan. *Physiol Plant* 116:164–171
- Thimm JC, Burritt DJ, Ducker WA, Melton LD (2009) Pectins influence microfibril aggregation in celery cell walls: an atomic force microscopy study. *J Struct Biol* 168:337–344
- Thompson DS (2005) How do cell walls regulate plant growth? *J Exp Bot* 56:2275–2285
- Turner BD, Henley BJ, Sleaf SB, Sloan SW (2015) Kinetic model selection and the Hill model in geochemistry. *J Environ Sci Technol* 12:2545–2558
- Verbelen JP, Vissenberg K (2007) *The expanding cell*. Springer, Berlin

- Villares A, Moreau C, Dammak A, Capron I, Cathala B (2015) Kinetic aspects of the adsorption of xyloglucan onto cellulose nanocrystals. *Soft Matter* 11:6472–6481
- Walesiuk M, Gantar E (2012) Statystyczna analiza danych z wykorzystaniem programu R. Wydawnictwo Naukowe PWN, Warszawa
- Wasewar KL, Atif M, Prasad B, Mani Mishra I (2008) Adsorption of zinc using tea factory waste: kinetics, equilibrium and thermodynamics. *Clean Soil Air Water* 36:320–329
- Willats WGT, Knox JP, Mikkelsen JD (2006) Pectin: new insights into an old polymer are starting to gel. *Trends Food Sci Technol* 17:97–104
- Winter HT, Cerclier C, Delorme N, Bizot H, Quemener B, Cathala B (2010) Improved colloidal stability of bacterial cellulose nanocrystal suspensions for the elaboration of spin-coated cellulose-based model surfaces. *Biomacromolecules* 10:3144–3151
- Zykwinska A, Ralet MC, Garnier C, Thibault JF (2005) Evidence for in vitro binding of pectin side chains to cellulose. *Plant Physiol* 139:396–407
- Zykwinska A, Thibault JF, Ralet MC (2008) Modelling of xyloglucan, pectins and pectic side chains binding onto cellulose microfibrils. *Carbohydr Polym* 74:23–30